npg

RESEARCH PAPER

Diazoxide acts more as a PKC-ε activator, and indirectly activates the mitochondrial K_{ATP} channel conferring cardioprotection against hypoxic injury

M-Y Kim[1,2], MJ Kim[1], IS Yoon[1], JH Ahn[1], SH Lee[1], EJ Baik[1], C-H Moon[1] and Y-S Jung[1,2]

[1]Department of Physiology, School of Medicine, Ajou University, Suwon, South Korea and [2]Department of Molecular Science and Technology, Ajou University, Suwon, South Korea

Background and purpose: Diazoxide, a well-known opener of the mitochondrial ATP-sensitive potassium (mitoK$_{ATP}$) channel, has been demonstrated to exert cardioprotective effect against ischemic injury through the mitoK$_{ATP}$ channel and protein kinase C (PKC). We aimed to clarify the role of PKC isoforms and the relationship between the PKC isoforms and the mitoK$_{ATP}$ channel in diazoxide-induced cardioprotection.

Experimental approach: In H9c2 cells and neonatal rat cardiomyocytes, PKC-ε activation was examined by Western blotting and kinase assay. Flavoprotein fluorescence, mitochondrial Ca^{2+} and mitochondrial membrane potential were measured by confocal microscopy. Cell death was determined by TUNEL assay.

Key results: Diazoxide (100 μM) induced translocation of PKC-ε from the cytosolic to the mitochondrial fraction. Specific blockade of PKC-ε by either εV1-2 or dominant negative mutant PKC-ε (PKC-ε KR) abolished the anti-apoptotic effect of diazoxide. Diazoxide-induced flavoprotein oxidation was inhibited by either εV1-2 or PKC-ε KR transfection. Treatment with 5-hydroxydecanoate (5-HD) did not affect translocation and activation of PKC-ε induced by diazoxide. Transfection with wild type PKC-ε mimicked the flavoprotein-oxidizing effect of diazoxide, and this effect was completely blocked by εV1-2 or 5-HD. Diazoxide prevented the increase in mitochondrial Ca^{2+}, mitochondrial depolarization and cytochrome c release induced by hypoxia and all these effects of diazoxide were blocked by εV1-2 or 5-HD.

Conclusions and Implications: Diazoxide induced isoform-specific translocation of PKC-ε as an upstream signaling molecule for the mitoK$_{ATP}$ channel, rendering cardiomyocytes resistant to hypoxic injury through inhibition of the mitochondrial death pathway.

British Journal of Pharmacology (2006) **149**, 1059–1070. doi:10.1038/sj.bjp.0706922; published online 16 October 2006

Introduction

Diazoxide, a well-known opener of the mitochondrial ATP-sensitive potassium (mitoK$_{ATP}$) channel, has been demonstrated to exert protective effects against ischemic injury in hearts and cardiomyocytes (Murata *et al.*, 2001; Zaugg *et al.*, 2002). Regarding the signaling mechanism for its cardioprotective effect, the mitoK$_{ATP}$ channel and protein kinase C (PKC) have been suggested as essential components (Sato *et al.*, 1998; Liu *et al.*, 2002; Ohnuma *et al.*, 2002). PKCs are classified into three subfamilies, which include the conventional (α, βI, βII, γ), novel (δ, ε, η, θ, ι) and atypical (ζ, μ, λ) isoforms based on Ca^{2+} and phospholipid sensitivity (Simkhovich *et al.*, 1998). Although the predominant isoforms in rat heart are α, β, δ, ε and ζ subtypes (Disatnik *et al.*, 1994), which PKC isoforms are essential for diazoxide-induced cardioprotection during hypoxia has not been thoroughly elucidated.

Furthermore, the nature of the interrelationship between PKC activation and the mitoK$_{ATP}$ channel opening in the mechanism of diazoxide-induced cardioprotection has not been clear. Previous studies suggest that PKC activation can modulate mitoK$_{ATP}$ channel activation (Sato *et al.*, 1998), based on the findings that the PKC activating phorbol ester

augmented activation of the mitoK$_{ATP}$ channel induced by diazoxide (Sato *et al.*, 1998), and that cardioprotection by diazoxide was abolished by a blockade of the mitoK$_{ATP}$ channel, but not by an inhibition of PKC (Ohnuma *et al.*, 2002). On the other hand, other studies showed that PKCs were translocated and/or activated in diazoxide-treated hearts and cardiomyocytes (Wang *et al.*, 1999; Liu *et al.*, 2002), suggesting that diazoxide-induced opening of the mitoK$_{ATP}$ channel is upstream of PKC activation.

The goal of the present study was to clarify the role of PKC isoforms and the relationship between the PKC isoforms and the mitoK$_{ATP}$ channel in diazoxide-induced cardioprotection in a hypoxic injury model of cardiomyocytes, by a pharmacological approach using PKC isoform-specific inhibitors and a molecular approach using transfection of wild-type or dominant-negative mutant form of the PKC-ε. In this study, rat heart-derived H9c2 cell lines (H9c2 cells) were used, as they are not only convenient but also recognized as a model well-suited for the study of cardiomyocyte biology (Hescheler *et al.*, 1991). To show the relevance of this cell line, some key experiments have been repeated in primary cultures of neonatal rat cardiomyocytes.

Materials and methods

Cell culture: primary culture of neonatal rat cardiomyocytes and cell line of H9c2

Cardiac ventricular myocytes were prepared from 1- to 2-day-old Sprague–Dawley rats as follows. The hearts were removed, and the ventricles were minced in calcium- and bicarbonate-free Hank's buffer with 2-[4-(2-hydroxyethyl)-1-piperazinyl]ethanesulfonic acid (HEPES). These tissue fragments were digested by stepwise 0.03% collagenase type II (Gibco BRL, Rockville, MD, USA) and 0.06% pancreatin (Sigma, St Louis, MO, USA). The dissociated cells were preplated for 1 h to enrich the culture with myocytes. The nonadherent myocytes were then plated at a density of 1.5×10^4 cells/mm^2. Rat heart-derived H9c2 cells were purchased from the American Type Culture Collection (ATCC, Rockville, MD, USA). Both types of cell were cultured before experimentation in Dulbecco's modified Eagle's medium containing 5.5 mM glucose supplemented with 10% fetal bovine serum and 1% penicillin/streptomycin. The cells were maintained at 37°C in the presence of 5% CO$_2$ in a water-jacked incubator gassed with 95% O$_2$ and 5% CO$_2$.

Hypoxic condition

For hypoxic challenges, the cells were transferred into an anaerobic chamber (Forma Scientific, Marietta, OH, USA) maintained at 37°C with a humidified atmosphere of 5% CO$_2$, 10% H$_2$ and 85% N$_2$ as previously described (Kim *et al.*, 2003). The anaerobic environment inside the chamber was monitored with diluted methylene blue solution as an O$_2$ indicator before and during experiments.

Soluble/particulate fractionation

Subcellular soluble/particulate fractionation of cells was performed by a method previously described (Kim *et al.*,

2003; Moon *et al.*, 2004). Briefly, the cells were lysed using lysis buffer (20 mM Tris-HCl (pH 7.4), 2 mM ethylenediamine-*N,N,N′,N′*-tetraacetic acid (EDTA), 5 mM ethylene glycol-bis-(2-aminoethyl ether)-*N,N,N′,N′*-tetraacetic acid (EGTA), 5 mM dithiothreitol, 6 mM *β*-mercaptoethanol, 1 mM phenyl-methylsulphonyl fluoride, 20 mM leupeptin, 50 μg/ml aprotinin). The particulate (membrane) and the soluble (cytosolic) fractions of the lysates were separated by centrifugation at 100 000 *g* for 1 h at 4°C, and the supernatant was collected for the soluble fraction. Pellets resuspended in the same volume of lysis buffer containing 1% Triton X-100 were centrifuged at 10 000 *g* for 10 min at 4°C, and the supernatant was collected for the particulate fraction.

Cytosolic/mitochondrial fractionation

Subcellular cytosolic/mitochondrial fractionation of cells was performed as previously described (Kim *et al.*, 2005). Briefly, the cells were collected by centrifugation at 1000 *g* for 10 min at 4°C. The cell pellets were resuspended in lysis buffer (20 mM HEPES-KOH (pH 7.5), 10 mM KCl, 1.5 mM MgCl$_2$, 1 mM sodium EDTA, 1 mM sodium EGTA, 1 mM dithiothreitol, 0.1 mM phenylmethylsulphonyl fluoride, 250 mM sucrose, 10 μg/ml leupeptin and 10 μg/ml aprotinin). The cells were then homogenized in a glass homogenizer, and the nuclei and cell debris were removed by centrifugation at 1000 *g* for 15 min at 4°C. The supernatants were further centrifuged at 10 000 *g* for 15 min at 4°C, and the resulting mitochondrial pellets were resuspended in lysis buffer. The supernatants created from the 10 000 *g* centrifugation were centrifuged once more at 100 000 *g* for 1 h at 4°C, and the supernatant was collected and designated the cytosolic fraction. We verified the mitochondrial fraction by using the mitochondrial marker, cytochrome oxidase subunit IV (COX), plasma membrane fraction with the dihydropyridine receptor protein (DRP) and cytosolic fractions with actin.

Western blotting

A quantity of 40 μg protein was separated on 8–15% sodium dodecyl sulphate–polyacrylamide gel electrophoresis (SDS–PAGE), and transferred onto polyvinylidene fluoride (PVDF) membrane (Millipore, Bedford, MD, USA). The membrane was blocked with 5% nonfat dry milk, and incubated with a primary antibody. The membrane was then incubated with a secondary immunoglobulin antibody conjugated with alkaline phosphate, and the band was visualized using the NBT/BCIP method (Sigma-Aldrich, St Louis, MO, USA).

In situ *terminal deoxynucleotidyl transferase UTP nick end labeling (TUNEL) assay*

To examine the extent of apoptotic cell death, we performed TUNEL-staining after 8 and 6 h of hypoxia in H9c2 cells and neonatal rat cardiomyocytes, respectively, as described previously (Jung *et al.*, 2003; Kim *et al.*, 2005). There are three groups of diazoxide treatment. (1) 'pre': the cells were treated with diazoxide 1 h before hypoxia followed by

washout during hypoxia. (2) 'during': the cells were treated with diazoxide only during hypoxia. (3) 'pre/during': the cells were treated with diazoxide 1 h before and during hypoxia.

Flavoprotein fluorescence

The cells were superfused with glucose-free Tyrode's solution containing the following: 140 mM NaCl, 5.4 mM KCl, 1.8 mM CaCl$_2$, 0.33 mM NaH$_2$PO$_4$, 0.5 mM MgCl$_2$ and 5 mM HEPES (pH 7.4). Flavoprotein fluorescence was excited at 480 nm (for 200 ms every 20 s) and emitted at 520 nm. Relative fluorescence was calibrated with signals recorded after exposure to 100 μM 2,4-dinitrophenol (DNP), which uncouples respiration from ATP synthesis, collapses the mitochondrial potential, and induces maximal oxidation. Therefore, the values of flavoprotein fluorescence were expressed as a percentage of the DNP-induced fluorescence.

Measurement of mitochondrial membrane potential

The mitochondrial membrane potential ($\Delta\psi_m$) was assayed by measuring the accumulation of rhodamine 123 (Molecular Probes, Eugene, OR, USA), a membrane-permeable cationic fluorescent dye (Emaus *et al.*, 1986). H9c2 cells were loaded with 1 μM rhodamine 123 in HEPES-buffered control salt solution (HCSS) containing 120 mM NaCl, 5 mM KCl, 1.6 mM MgCl$_2$, 2.3 mM CaCl$_2$, 15 mM glucose, 20 mM HEPES and 10 mM NaOH. The cells were incubated for 10 min at 37°C and washed three times with HCSS. The fluorescence intensity of the cell was then measured by flow cytometry (BD Biosciences, Oxford, UK).

Measurement of mitochondrial Ca^{2+} uptake

The mitochondrial Ca^{2+} level ([Ca^{2+}]$_{mito}$) was quantified after loading cells with the Ca^{2+} fluorophore rhod-2 (Molecular Probes, Eugene, OR, USA), a selective fluorescent indicator for mitochondrial Ca^{2+}. Mitochondria were labeled with 100 nM Green Mito-Tracker (Molecular probes, Eugene, OR, USA). For double-labeling, H9c2 cells were incubated for 10 min in HCSS at 37°C with 100 nM Green Mito-Tracker. The 2-step cold loading/warm incubation protocol achieves exclusive loading of rhod-2 into the mitochondria (Trollinger *et al.*, 1997). Rhod-2 fluorescence was excited at 560 nm and emitted fluorescence was collected through a 590-nm-long pass barrier filter. The fluorescence intensity of rhod-2 was quantified using image-analysis computer software (Fluoview FV300; Olympus, Japan).

Plasmid construction

Wild-type PKC-ε (PKC-ε WT) and the dominant-negative mutant form of PKC-ε (PKC-ε KR) were cloned into pHACE that contains N-terminal HA tag (Lee *et al.*, 2003). PKC-ε WT constructs contained the full-length open reading frames of PKC-ε and PKC-ε KR constructs contained full-length open reading frame with a K→R point mutation in the ATP binding site.

Cell transfection

H9c2 cells were transiently transfected with either empty vector as a control (pcDNA3) or various expression vectors using Lipofectin (Invitrogen, Carlsbad, CA, USA), following the procedure recommended by the manufacturer. The cells were grown to 50∼60% confluence before transfection. The pHACE-PKC-ε DNA construct was mixed with the Lipofection reagent. The mixture was then added to the serum-free cell culture medium and incubated at 37°C for 8 h, which was followed by transfection to the cells.

PKC-ε kinase assay

Cellular proteins were extracted using PKC extraction buffer (50 mM HEPES (pH 7.5), 150 mM NaCl, 0.1% Tween 20, 1 mM EDTA, 2.5 mM EGTA and 10% glycerol) containing protease inhibitors (10 μg/ml each of aprotinin and leupeptin and 0.1 mM phenylmethylsulphonyl fluoride) and phosphatase inhibitors (1 mM NaF, 0.1 mM Na$_3$VO$_4$ and 10 mM β-glycerophosphate). HA-tagged PKC proteins from 500 μg of cell extracts were immunoprecipitated with 3 μg of anti-HA antibody and 30 μl of protein G-Sepharose for 3 h at 4°C. The immunoprecipitates were resuspended in PKC reaction buffer (50 mM HEPES (pH 7.5), 10 mM MgCl$_2$, 1 mM dithiothreitol, 2.5 mM EGTA, 1 mM NaF, 0.1 mM Na$_3$VO$_4$ and 10 mM β-glycerophosphate). The kinase assay was initiated by adding PKC reaction buffer containing 5 μg of PKC-ε substrate and 5 μCi of [γ-^{32}P]ATP. Reactions were carried out for 30 min at 37°C and terminated by adding sodium dodecyl sulfate (SDS) sample buffer. Mixtures were then boiled for 5 min, and the reaction products were analyzed by SDS–polyacrylamide gel electrophoresis (PAGE) and autoradiography.

Statistical analysis

All data were expressed as mean ± s.d. The numerical data were compared using a one-way analysis of variance followed by a post-test such as Bonferoni test. A P-value of <0.05 was considered significant.

Antibodies and drugs

Myristoylated PKC εV1–2 (εV1–2; an inhibitor of PKC-ε) was purchased from Biomol Research Lab (Plymouth Meeting, PA, USA). Diazoxide, 5-hydroxydecanoate (5-HD; a specific inhibitor of mitoK$_{ATP}$ channel), cyclosporin A (CsA; a permeability transition pore (PTP) inhibitor) and DNP (metabolic uncoupler) were purchased from Sigma (St Louis, MO, USA). Ruthenium Red (RR; an inhibitor of mitochondrial Ca^{2+} uniporter) was obtained from TOCRIS (Ellisville, MO, USA). Anti-PKC-α, -βI, -δ, -ε, -ζ (1:500) and anti-HA (1:500) antibodies were purchased from Santa Cruz Biotechnology (Santa Cruz, CA, USA). Anti-actin (1:3000) and anti-DRP (1:1000) antibodies were from Sigma (St Louis, Mo, USA). Anti-COX (1:3000) antibody was from Molecular Probes (Eugene, OR, USA). Diazoxide, εV1–2, CsA, and RR were dissolved in dimethyl sulfoxide (DMSO) to form stock solutions. The final DMSO concentration of 0.1% was found to have no effect on neonatal rat cardiomyocytes and H9c2

cell viability. The concentrations of inhibitors and treatments were chosen on the basis of preliminary studies (data not shown).

Results

Effect of diazoxide on PKC isoforms

Figures 1a and 2a show isoform-specific translocation of PKC-ε by diazoxide in H9c2 and neonatal rat cardiomyocytes, respectively. In both cells, the level of PKC-ε in the particulate fraction started to increase as early as 5 min and reached a peak at 30 min after treatment with diazoxide (100 μM). The level of PKC-ε in the soluble fraction was markedly decreased. The other PKC isoforms (PKC-α, -βI, -δ, -ζ) were not altered by diazoxide treatment in either the particulate or the soluble fractions. To evaluate whether diazoxide-induced translocation of PKC-ε involves mitochondrial translocation, we evaluated protein expression of PKC-ε in the mitochondrial fraction as well as the cytosolic fraction. As shown in Figures 1b and 2b, the cellular

subfractions, in terms of the mitochondrial, as well as the cytosolic and the plasma membrane fractions, were characterized by their specific markers, COX, actin and DRP, and no cross-contamination was found between the cellular fractions. The level of PKC-ε in the mitochondrial fraction increased at 5 min after 100 μM diazoxide treatment while levels in the cytosolic fractions were decreased remarkably (Figures 1b and c, 2b and c). The activity of PKC-ε in the mitochondrial fraction began to increase as early as 5 min after diazoxide treatment, with a maximal increase after 10 min, in H9c2 cells and neonatal rat cardiomyocytes (Figures 1d and 2d).

The role of PKC-ε in diazoxide-induced cardioprotection against apoptotic cell death during hypoxia

To investigate the role of translocated PKC-ε to the mitochondria induced by diazoxide, we examined the effect of specific blockade of PKC-ε translocation by εV1–2 on apoptotic cell death after 8 h of hypoxia in both H9c2 cells (Figure 3a and b) and 6 h of hypoxia in neonatal rat
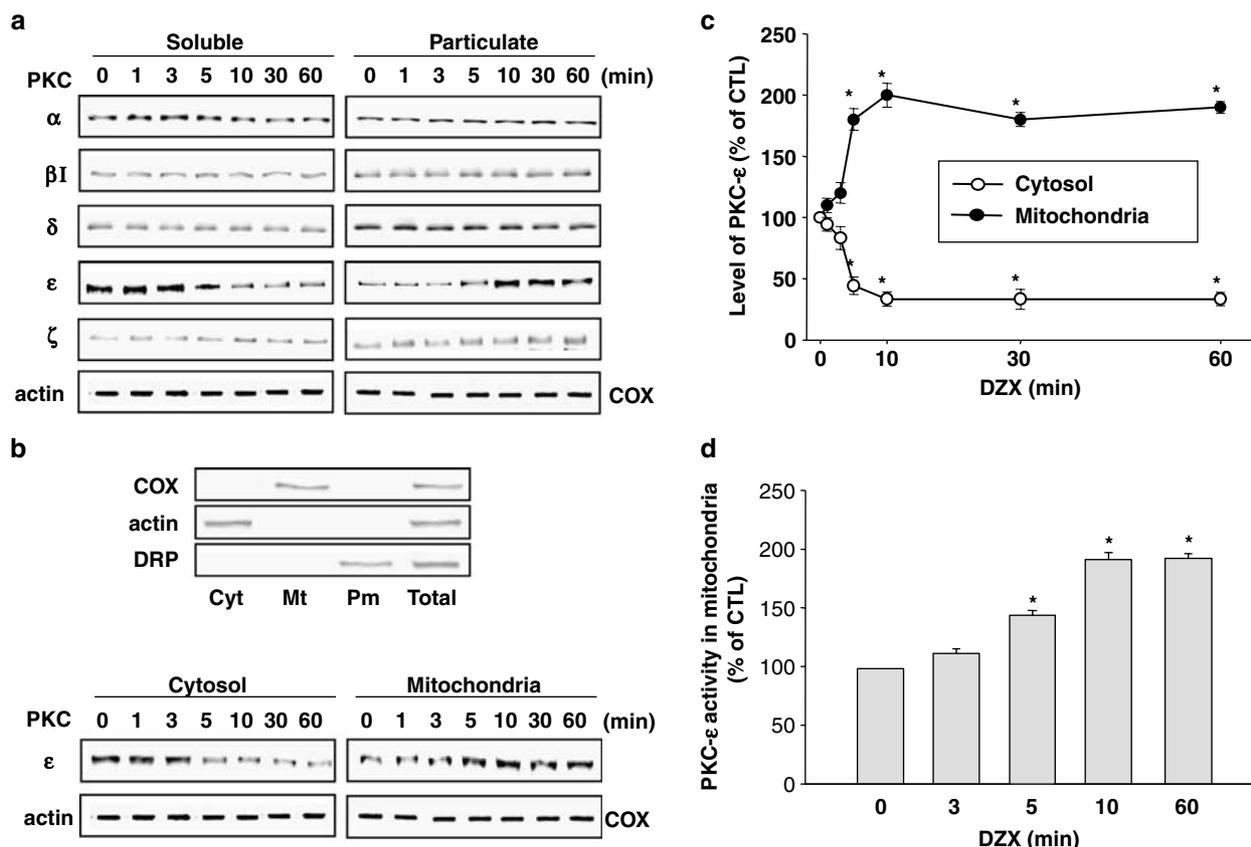

Figure 1 Effect of diazoxide (DZX) on PKC isotypes in H9c2 cells. (**a**) Western blots for PKC isotypes (-α, -βI, -δ, -ε and -ζ) detected in the soluble and the particulate fraction after various periods of diazoxide treatment. Data shown are representative of four separate experiments. COX, cytochrome *c* oxidase subunit IV. (**b**) Western blots for PKC-ε detected in cytosolic and the mitochondrial fraction after various periods of diazoxide treatment (lower panel). Western blots for subcellular markers, cytochrome *c* oxidase subunit IV (COX), dihydropyridine receptor protein (DRP) and actin (upper panel). Data shown are representative of four separate experiments. Cyt, cytosol; Mt, mitochondria; Pm, plasma membrane. (**c**) Quantitative analysis for PKC-ε in the cytosolic and the mitochondrial fraction after various periods of diazoxide treatment. Data shown as means±s.d. (*n*=4) represent the percentage of the control (CTL, 0 time). *$P<0.05$ vs vehicle-treated control (CTL, 0 time). (**d**) Kinase activity for PKC-ε measured in mitochondrial fraction after various periods of diazoxide treatment. Data shown as means±s.d. (*n*=4) represent the percentage of the control (CTL, 0 time). *$P<0.05$ vs vehicle-treated control (CTL, 0 time).

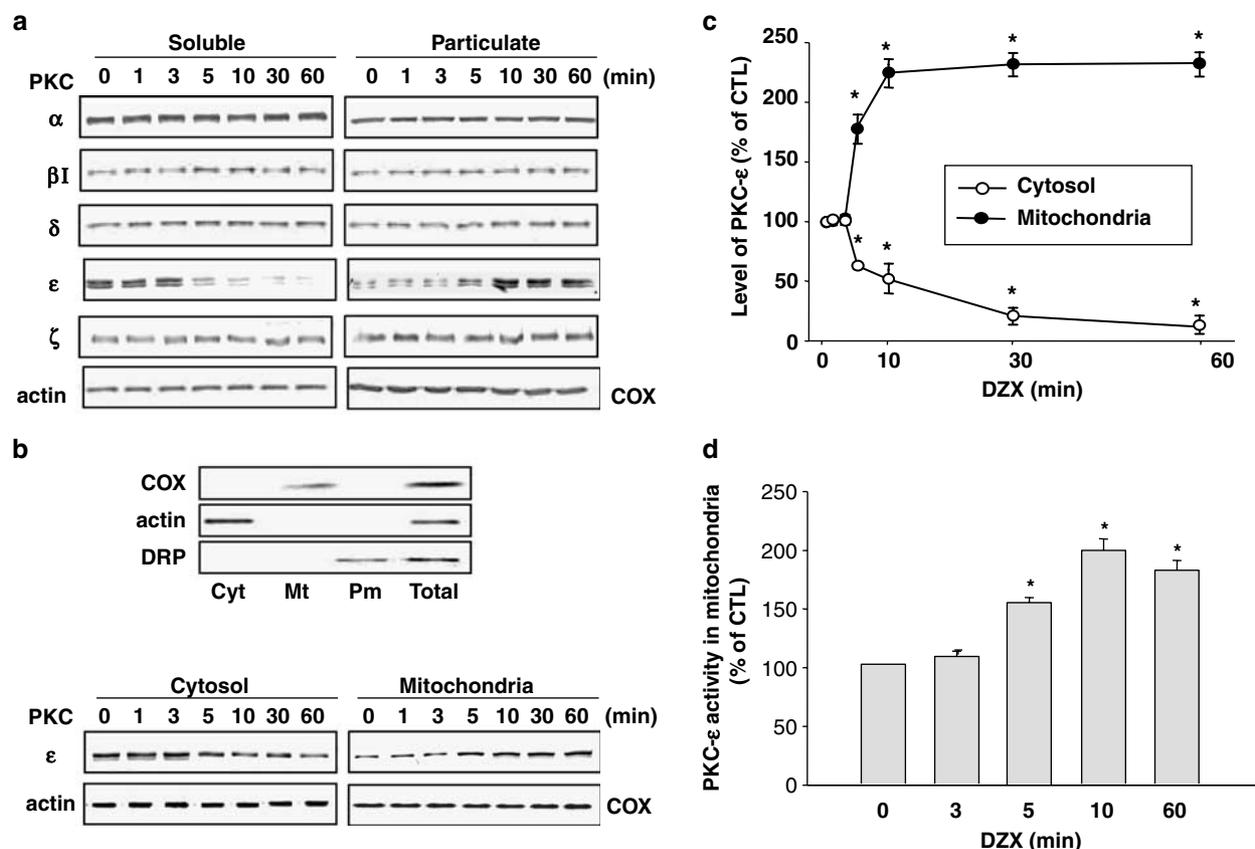Diazoxide acts as a PKC-ε activator
M-Y Kim et al
1063

Figure 2 Effect of diazoxide (DZX) on PKC isotypes in neonatal rat cardiomyocytes. (**a**) Western blots for PKC isotypes (-α, -βI, -δ, -ε and -ζ) detected in the soluble and the particulate fraction after various periods of diazoxide treatment. Data shown are representative of four separate experiments. COX, cytochrome c oxidase subunit IV. (**b**) Western blots for PKC-ε detected in cytosolic and the mitochondrial fraction after various periods of diazoxide treatment (lower panel). Western blots for subcellular markers, cytochrome c oxidase subunit IV (COX), dihydropyridine receptor protein (DRP) and actin (upper panel). Data shown are representative of four separate experiments. Cyt, cytosol; Mt, mitochondria; Pm, plasma membrane. (**c**) Quantitative analysis for PKC-ε in the cytosolic and the mitochondrial fraction after various periods of diazoxide treatment. Data shown as means $\pm$ s.d. ($n=4$) represent the percentage of the control (CTL, 0 time). *$P<0.05$ vs vehicle-treated control (CTL, 0 time). (**d**) Kinase activity for PKC-ε measured in mitochondrial fraction after various periods of diazoxide treatment. Data shown as means $\pm$ s.d. ($n=4$) represent the percentage of the control (CTL, 0 time). *$P<0.05$ vs vehicle-treated control (CTL, 0 time).

cardiomyocytes (Figure 3d and e). Periods of hypoxia, producing about 50% of cell death, were determined by preliminary experiment (data not shown), and differences between the two cell types appears due to the greater tendency of the neonatal rat cardiomyocytes to detach from the culture plate and their shorter time course of cell death compared to H9c2 cells. The proportion of TUNEL-positive cells after 8 h of hypoxia in H9c2 cells, and that after 6 h of hypoxia in neonatal rat cardiomyocytes was the same, about 30–35% (Figure 3a and d). The TUNEL-positive cells in both cultures were attenuated by diazoxide treatment in the 'pre/during' group, but not in the 'pre' nor in the 'during' group. The anti-apoptotic effect of diazoxide (Figure 3b and e) was almost completely blocked by 10 μM εV1–2 and by 100 μM 5-HD. These results suggest the involvement of PKC-ε as well as mitoK$_{ATP}$ channel in the mechanism of diazoxide-induced cardioprotection. Consistent with these results, Figure 3c (H9c2 cells) and f (neonatal rat cardiomyocytes) show that a high level of PKC-ε in the mitochondrial fraction of diazoxide-treated group was maintained, up to 2 h of hypoxia, while the protein levels of PKC-ε in both the cytosolic and the mitochondrial fraction (Kim *et al.*, 2003)

were diminished after 2 h of hypoxia in the hypoxic control cultures.

As shown in Figure 4a, the expression vectors for PKC-ε WT or PKC-ε KR were transfected into H9c2 cells, to verify that they expressed the predicted protein (HA), and the constructs were found to express the corresponding proteins with expected sizes at comparable levels. In addition, increased kinase activity of PKC-ε was found in PKC-ε WT transfected cells and decreased PKC-ε kinase activity was shown in PKC-ε KR transfected cells (Figure 4b). As shown in Figure 4c, in cells transfected with pcDNA3, about 28% was shown as TUNEL-positive after 8 h of hypoxia. This increase in TUNEL-positive cells was dramatically attenuated by diazoxide treatment or by transfection of PKC-ε WT. The anti-apoptotic effect of diazoxide during hypoxia was almost completely blocked in PKC-ε KR transfected cells.

Link between PKC-ε and the mitoK$_{ATP}$ channel
To investigate the link between PKC-ε and the mitoK$_{ATP}$ channel, we examined the effect of 5-HD on PKC-ε translocation and the effect of εV1–2 on mitoK$_{ATP}$ channel
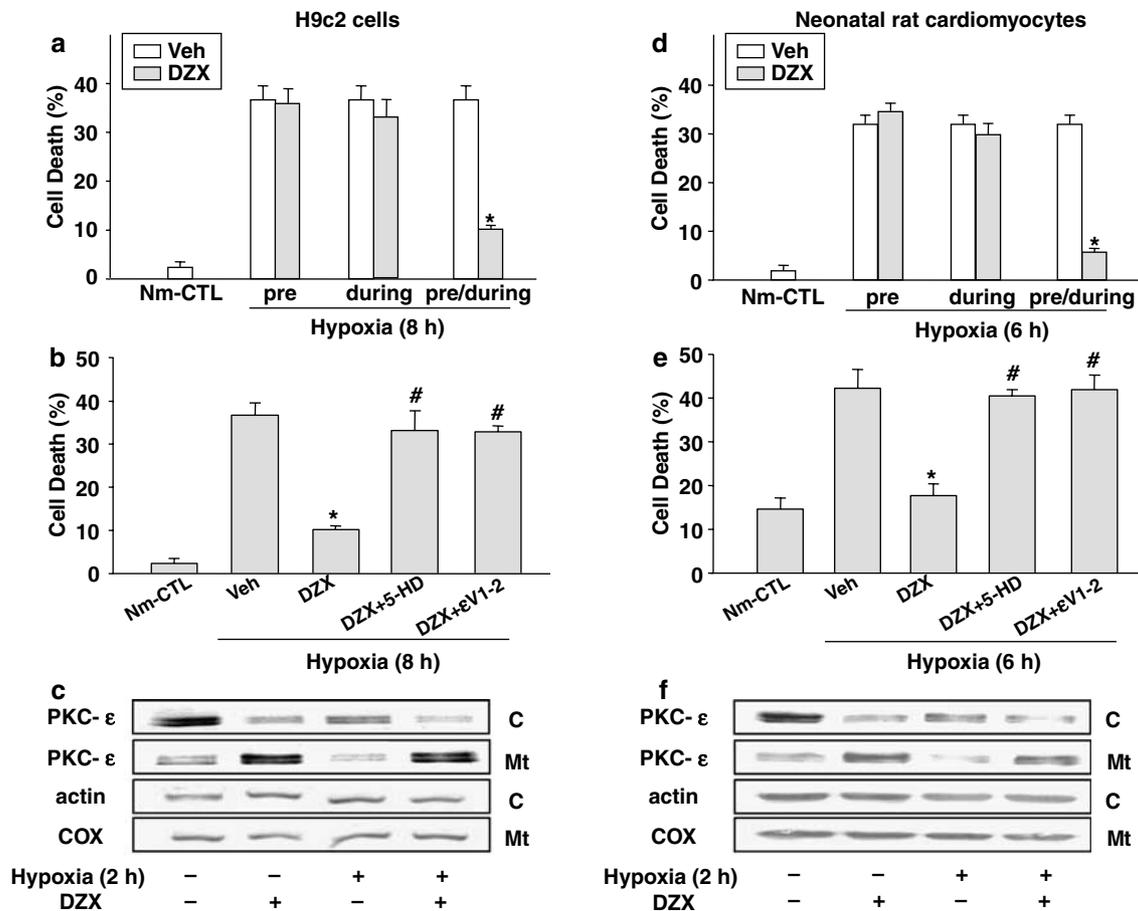
Figure 3 The role of PKC-ε in diazoxide-induced cardioprotection against hypoxia-induced apoptotic cell death in H9c2 cells (a–c) and in neonatal rat cardiomyocytes (d–f). (a and d) Effect of diazoxide (DZX) on hypoxia-induced apoptotic cell death. The cells were treated with 100 μM diazoxide 1 h before hypoxia ('pre'), during hypoxia ('during') or 1 h before and during hypoxia ('pre/during'). Cell death (%) was calculated by dividing the number of TUNEL-stained cells by total number of cells 8 h (a) and 6 h (d) after hypoxic insult. The data are mean ± s.d. ($n = 5$). *$P < 0.05$ vs vehicle-treated hypoxic control (Veh). Nm-CTL, vehicle-treated normoxic control. (b and e) Effect of PKC-ε inhibitor (εV1–2) and mitoK$_{ATP}$ channel inhibitor (5-HD) on diazoxide-induced cardioprotection against hypoxia-induced apoptotic cell death. The cells were treated with 100 μM diazoxide 1 h before and during hypoxia in the absence or presence of 10 μM εV1–2 or 100 μM 5-HD. Cell death (%) was calculated by dividing the number of TUNEL-stained cells by total number of cells 8 h (b) and 6 h (e) after hypoxic insult. The data are mean ± s.d. ($n = 5$). *$P < 0.05$ vs vehicle-treated hypoxic control (Veh), #$P < 0.05$ vs diazoxide-treated hypoxia (DZX). Nm-CTL, vehicle-treated normoxic control. (c and f) Effect of diazoxide on PKC-ε expression during hypoxia. The cells were treated with 100 μM diazoxide for 1 h before and during hypoxia. Western blots for PKC-ε detected in the cytosolic (C) and the mitochondrial (Mt) fractions after 2 h of hypoxia. Data shown are representative of four separate experiments. COX, cytochrome c oxidase subunit IV.

activation, monitored by flavoprotein oxidation. Opening of mitoK$_{ATP}$ channels dissipates the inner $\Delta\psi_m$ established by the proton pump. This dissipation accelerates electron transfer by the respiratory chain and if uncompensated by increased production of electron donors, leads to net oxidation of the mitochondria. We therefore monitored the mitochondrial redox state by recording the fluorescence of flavoprotein in the mitochondria as an indirect index of the mitoK$_{ATP}$ channel opening (Liu et al., 1998; Wang et al., 2001a). Figures 5a and 6a show the time course of changes in flavoprotein fluorescence in H9c2 cells and neonatal rat cardiomyocytes exposed to diazoxide. Flavoprotein fluorescence began to increase as early as 7 min after diazoxide treatment, with a resultant plateau at about 10 min. Consistent with earlier reports (Liu et al., 1998), these diazoxide-induced flavoprotein oxidations were completely inhibited by 5-HD to control level in both types of cell. As shown in

Figures 5b and 6b, the maximum flavoprotein oxidations by diazoxide were completely blocked by 10 μM εV1–2. When we investigated the effect of 5-HD on PKC-ε translocation, diazoxide-induced PKC-ε translocation to mitochondria remained unaltered after 5-HD treatment in both H9c2 cells and neonatal rat cardiomyocytes (Figures 5c and 6c). The kinase activity of PKC-ε in the mitochondrial fraction was almost doubled by treatment with diazoxide (Figures 5d and 6d). This increase was blocked by 10 μM εV1–2 but not by 5-HD, in both H9c2 cells and neonatal rat cardiomyocytes.

On the basis of these results, the role of specific translocation of PKC-ε by diazoxide in hypoxic cell death and the interrelationship between PKC-ε and the mitoK$_{ATP}$ channel were shown to be quite similar each other in both H9c2 cells and neonatal rat cardiomyocytes. We therefore performed the following experiments using only the more convenient H9c2 cells.
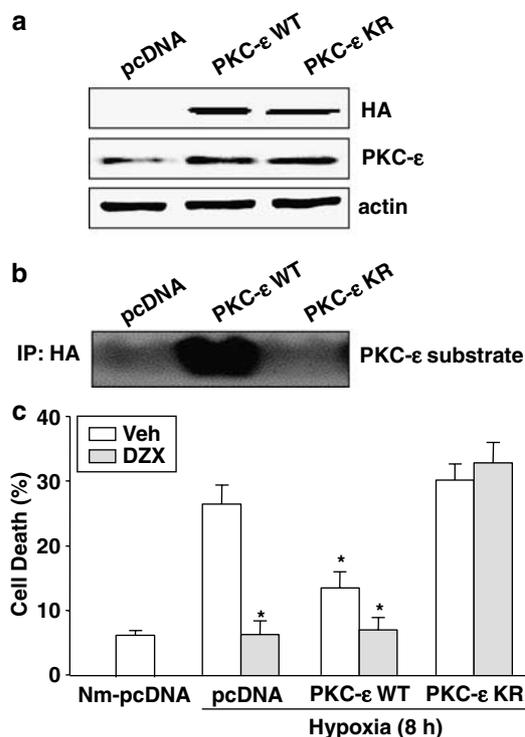
Figure 4 The role of PKC-ε in diazoxide-induced cardioprotection against hypoxia-induced apoptotic cell death in PKC-ε transfected cells. H9c2 cells were transfected with PKC-ε sequence (PKC-ε WT or PKC-ε KR) vector and control vector pcDNA3. (**a**) Western blots for HA or PKC-ε detected in the PKC-ε transfected cells. Data shown are representative of four separate experiments. (**b**) Kinase activity for PKC-ε measured in the PKC-ε transfected cells. Data shown are representative of four separate experiments. (**c**) The role of PKC-ε in diazoxide-induced cardioprotection against hypoxia-induced apoptotic cell death. The PKC-ε transfected cells were treated with or without 100 μM diazoxide (DZX) 1 h before and during hypoxia. Cell death (%) was calculated by dividing the number of TUNEL-stained cells by total number of cells 8 h after hypoxic insult. The data are mean±s.d. ($n = 4$). *$P < 0.05$ vs vehicle-pcDNA, Nm, normoxia.

Effect of PKC-ε on mitoK$_{ATP}$ channel opening in PKC-ε transfected cells

In order to confirm the link between PKC-ε and mitoK$_{ATP}$ channel, we further examined the effect of direct PKC-ε activation or inactivation on flavoprotein oxidation, with H9c2 cells transfected with PKC-ε WT or PKC-ε KR. In cells transfected with PKC-ε WT, flavoprotein fluorescence was increased before diazoxide treatment and increased further after diazoxide treatment (Figure 7a and b). Maximum flavoprotein oxidation induced by diazoxide was markedly blocked in cells transfected with the negative mutant, PKC-ε KR (Figure 7a and b). Figure 7c shows that overexpression of PKC-ε WT-induced increase in flavoprotein oxidation was completely blocked by 5-HD, as well as by εV1–2.

The role of PKC-ε in diazoxide-induced inhibitory effect on mitochondrial death pathway

To elucidate the role of the PKC-ε in mitochondrial death pathway during hypoxia, we measured [Ca^{2+}]$_{mito}$, $\Delta\psi_m$ and cytochrome c release from the mitochondria to the cytosol

during hypoxia in H9c2 cells. As demonstrated in our previous results, hypoxia-induced elevation of [Ca^{2+}]$_{mito}$, and disruption of $\Delta\psi_m$ reaches peak at 1 and 4 h of hypoxia, respectively, and the level of cytochrome c released into cytosol reaches peak at 6 h of hypoxia (Kim *et al.*, 2005). Hypoxia-induced [Ca^{2+}]$_{mito}$ elevation and $\Delta\psi_m$ reduction was almost completely blocked by RR, but not by CsA (Figure 8a and b), suggesting that hypoxia-induced $\Delta\psi_m$ reduction is dependent on [Ca^{2+}]$_{mito}$ elevation rather than PTP opening. As expected, hypoxia-induced cytochrome c release was inhibited by CsA. Figure 8b shows that diazoxide-induced reduction of $\Delta\psi_m$ was completely abolished by 10 μM εV1–2 to control levels (Veh). As shown in Figure 8a–c, the treatment with diazoxide prevented the increase in [Ca^{2+}]$_{mito}$, mitochondrial depolarization and cytochrome c release induced by hypoxia, and all these effects of diazoxide were almost completely blocked by εV1–2 as well as 5-HD.

Discussion

The main findings of this study are that diazoxide-induced isoform-specific activation of PKC-ε is an intermediate step in the opening of the mitoK$_{ATP}$ channel, resulting in cardioprotection against hypoxia-induced death in H9c2 cells and neonatal rat cardiomyocytes.

This study demonstrates that diazoxide induces isoform-specific translocation of PKC-ε from the soluble to the particulate, especially to the mitochondrial fraction, and that diazoxide increases PKC-ε activity in the mitochondrial fraction in H9c2 cell lines and primary culture of neonatal rat cardiomyocytes (Figures 1 and 2). This study further shows that measurable protein levels and activities of PKC-ε can be detected in the mitochondrial fraction in the absence of diazoxide (Figures 1d and 2d), suggesting the existence of PKC-ε inside mitochondria in the basal state. Consistent with our results, recent reports demonstrated that PKC-ε exists constitutively inside mitochondria, but only equivalent to 10–20% of that observed in the cytosol in the basal state and that PKC-ε is either very tightly bound or, more likely, is localized in the intermembrane space in heart mitchondria (Baines *et al.*, 2002; Costa *et al.*, 2005).

The results obtained from the pharmacological and the molecular approach using εV1–2, and a dominant-negative mutant form of PKC-ε, suggest the essential role of PKC-ε activation in diazoxide-induced cardioprotection (Figures 3b, e and 4c). Although these results are not consistent with previous studies in rat heart, suggesting that diazoxide-induced translocation of PKC-δ is associated with cardioprotection (Wang and Ashraf, 1999; Wang *et al.*, 2001b), there are reports consistent with ours, suggesting a role for PKC-ε in diazoxide-induced cardioprotection in chick cardiomyocytes (Liu *et al.*, 2002). Other pharmacological actions of diazoxide have been known to include inhibition of succinate dehydrogenase (SDH) (Schafer *et al.*, 1969); the present study, however, did not consider the contribution of SDH inhibition to diazoxide-induced cardioprotection, because the concentration of diazoxide used in our study was much lower (100 μM) than that needed to achieve SDH
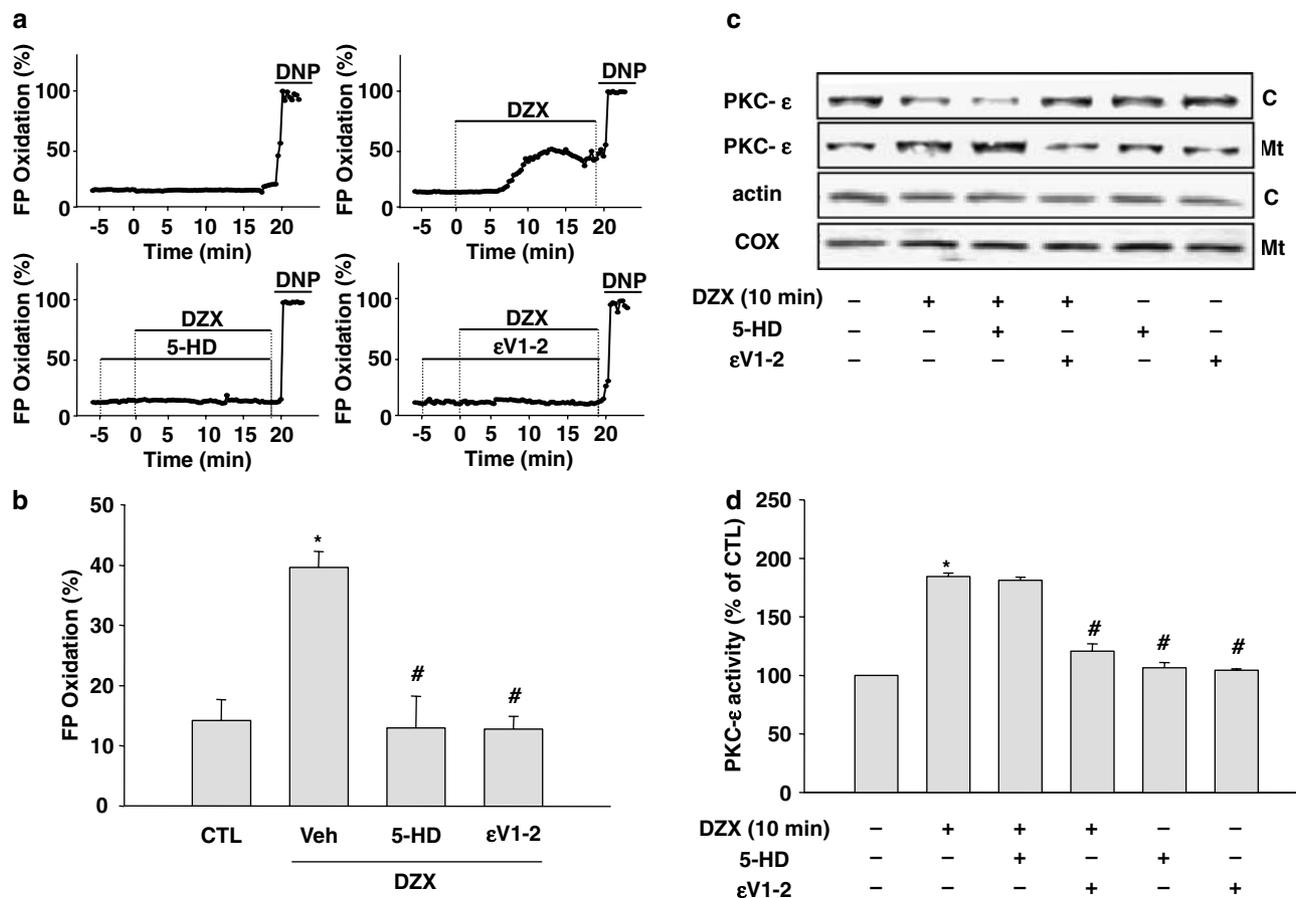
Figure 5 Link between PKC-ε and the mitoK$_{ATP}$ channel in H9c2 cells. The cells were treated with 100 μM diazoxide (DZX) in the absence or presence of PKC-ε inhibitor (εV1–2) or mitoK$_{ATP}$ channel inhibitor (5-HD). (**a**) Effect of 10 μM εV1–2 and 100 μM 5-HD on diazoxide-induced flavoprotein (FP) oxidation. FP oxidation (%) was calculated as a percentage of the 100 μM DNP-induced fluorescence. Data shown are representative of four separate experiments. (**b**) Effect of 10 μM εV1–2 and 100 μM 5-HD on diazoxide-induced maximum flavoprotein (FP) oxidation. FP oxidation (%) was calculated as a percentage of the 100 μM DNP-induced fluorescence. The data are mean$\pm$s.d. ($n=4$). *$P<0.05$ vs control (CTL), #$P<0.05$ vs diazoxide alone (Veh). (**c**) Effect of 10 μM εV1–2 and 100 μM 5-HD on diazoxide-induced translocation of PKC-ε. Western blots for PKC-ε detected in the cytosolic (C) and the mitochondrial (Mt) fractions after 10 min of diazoxide. Data shown are representative of four separate experiments. COX, cytochrome *c* oxidase subunit IV. (**d**) Effect of 10 μM εV1–2 and 100 μM 5-HD on diazoxide-induced increase of kinase activity of PKC-ε in mitochondria. The data are mean$\pm$s.d. ($n=4$). *$P<0.05$ vs vehicle-treated control (CTL), #$P<0.05$ vs DZX alone.

inhibition ($\sim 400\,\mu$M) (Schafer *et al.*, 1969; Grimmsmann and Rustenbeck, 1998).

As in the case of our previous study with KR-31378, a novel K$_{ATP}$ opener (Moon *et al.*, 2004), the cardioprotective effect of diazoxide was observed only in the 'pre/during' group and not in the 'pre' or the 'during' group (Figure 3a and d). These results are inconsistent with other studies showing that cardioprotective efficacy was still demonstrable when diazoxide treatment was commenced during reperfusion (Hausenloy *et al.*, 2004) or only before exposure to H$_2$O$_2$ (Akao *et al.*, 2003). These discrepancies cannot be readily explained, but may be due to different environments between *in vivo* and *in vitro* systems, and injury types.

From our results that 'pre/during' treatment with diazoxide exerts cardioprotection, involving PKC-ε and the mitoK$_{ATP}$ channel, we would suggest that the modulation of PKC-ε and the mitoK$_{ATP}$ channel by diazoxide should precede hypoxic insult and be maintained during hypoxia. These results prompted us to investigate further the relation-

ship between PKC-ε activation and the mitoK$_{ATP}$ channel opening, in the presence of diazoxide, before hypoxia. Our findings showed that blockade of PKC-ε by εV1–2 or dominant-negative mutant form of PKC-ε inhibited diazoxide-induced flavoprotein oxidation (Figure 3b and e), while diazoxide-induced PKC-ε translocation and activation remained unaltered after blockade of the mitoK$_{ATP}$ channel by 5-HD (Figure 3b–d and f). Based on these results, we would propose two possible signaling schemes: one, in which the signaling pathways for diazoxide-induced mitoK$_{ATP}$ channel opening and PKC-ε activation are independent of each other, and the other, in which diazoxide-induced PKC-ε activation occurs upstream of the activation of the mitoK$_{ATP}$ channel. Although we cannot exclude the possibility of independent signaling pathways for PKC-ε and the mitoK$_{ATP}$ channel, several pieces of evidence favor the latter, sequential, pathway. First, because either εV1–2 or 5-HD could completely, rather than partially, block the flavoprotein oxidizing effect of diazoxide (Figures 5a,b and 6a,b), it is
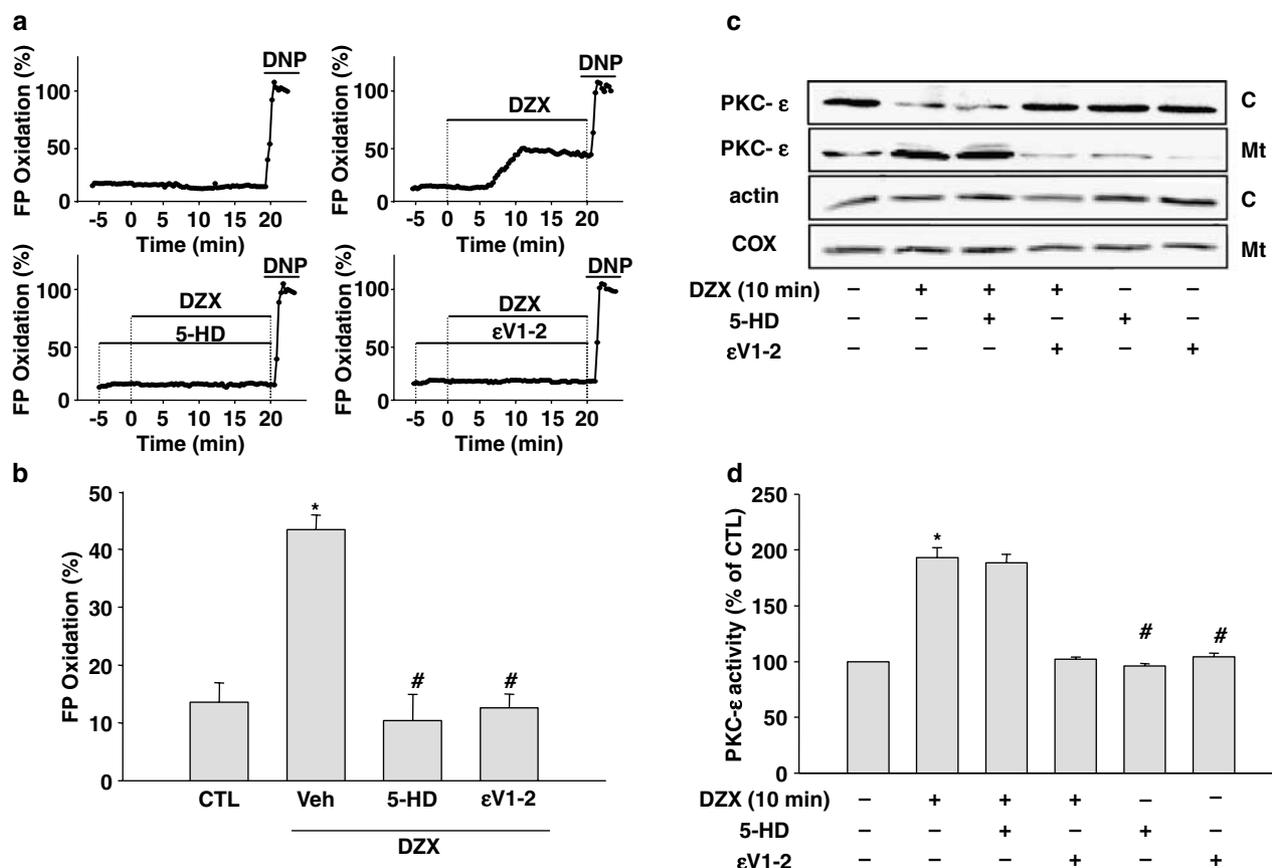
Figure 6 Link between PKC-ε and the mitoK$_{ATP}$ channel in neonatal rat cardiomyocytes. The cells were treated with 100 μM diazoxide (DZX) in the absence or presence of PKC-ε inhibitor (εV1–2) or mitoK$_{ATP}$ channel inhibitor (5-HD). (a) Effect of 10 μM εV1–2 and 100 μM 5-HD on diazoxide-induced flavoprotein (FP) oxidation. FP oxidation (%) was calculated as a percentage of the 100 μM DNP-induced fluorescence. Data shown are representative of four separate experiments. (b) Effect of 10 μM εV1–2 and 100 μM 5-HD on diazoxide-induced maximum flavoprotein (FP) oxidation. FP oxidation (%) was calculated as a percentage of the 100 μM DNP-induced fluorescence. The data are mean ± s.d. (n = 4). *$P < 0.05$ vs control (CTL), #$P < 0.05$ vs diazoxide alone (Veh). (c) Effect of 10 μM εV1–2 and 100 μM 5-HD on diazoxide-induced translocation of PKC-ε. Western blots for PKC-ε detected in the cytosolic (C) and the mitochondrial (Mt) fractions after 10 min of diazoxide. Data shown are representative of four separate experiments. COX, cytochrome *c* oxidase subunit IV. (d) Effect of 10 μM εV1–2 and 100 μM 5-HD on diazoxide-induced increase of kinase activity of PKC-ε in mitochondria. The data are mean ± s.d. (n = 4). *$P < 0.05$ vs vehicle-treated control (CTL), #$P < 0.05$ vs DZX alone.

likely that diazoxide-induced PKC-ε activation and mitoK$_{ATP}$ channel-dependent flavoprotein oxidation share the same signaling pathway. The partial inhibitory effect of transfection with PKC-ε KR mutant on the flavoprotein oxidizing effect of diazoxide may be due to the contribution of endogenous normal PKC-ε in the presence of diazoxide (Figure 7a and b). Second, direct activation of PKCs by overexpression of PKC-ε WT mimicked the flavoprotein oxidizing effect of diazoxide (Figure 7a), which was completely blocked by 5-HD, suggesting a signaling cascades of: PKC-ε→mitoK$_{ATP}$ channel→flavoprotein oxidation. Third, as judged from the time course results, because diazoxide-induced PKC-ε translocation reached its maximum level at 5 min (Figures 1 and 2) and the corresponding flavoprotein oxidation was maximal at about 10 min (Figures 5a and 6a), it is likely that mitoK$_{ATP}$ channel-dependent flavoprotein oxidation occurs downstream of PKC-ε activation. Taken together, these considerations lead us to suggest that diazoxide first induces isoform-specific translocation of

PKC-ε into mitochondria, which in turn activates the mitoK$_{ATP}$ channel located on the inner mitochondrial membrane. Translocation of the cytosolic PKC-ε to the mitochondria by diazoxide seems to be essential for PKC-ε to link with the mitoK$_{ATP}$ channel, leading to the mitoK$_{ATP}$ channel opening. In addition, mitochondrial localization of PKC-ε in the basal state provides another possibility for PKC-ε to link with the mitoK$_{ATP}$ channel in the presence of diazoxide, leading to the mitoK$_{ATP}$ channel opening.

It has been known that during hypoxia, cytosolic Ca^{2+} increases and mitochondria takes up some of the increased cytosolic Ca^{2+} through a RR-sensitive Ca^{2+} uniporter (Anderson *et al.*, 2005), which in turn induces the opening of PTP, and the disruption of the Δψ$_m$, leading to release of cytochrome *c*, caspase-3 activation and apoptotic cell death (Gunter *et al.*, 1994). Supporting this notion, our study confirmed that hypoxia-induced [Ca^{2+}]$_{mito}$ elevation and Δψ$_m$ reduction were almost completely blocked by RR (Figure 8a and b). From the results using CsA, an inhibitor of PTP
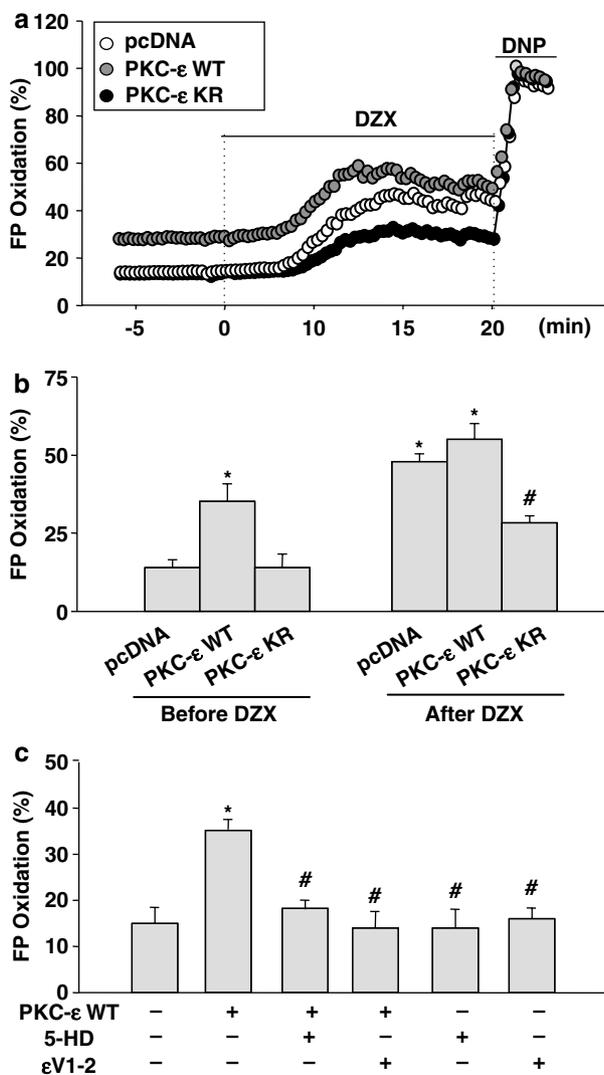
Figure 7 Link between PKC-ε and the mitoK$_{ATP}$ channel in PKC-ε transfected cells. The H9c2 cells were transfected with PKC-ε sequence (PKC-ε WT and PKC-ε KR) vector and control vector pcDNA3. (**a**) Effect of transfection of PKC-ε on diazoxide-induced flavoprotein (FP) oxidation. The PKC-ε transfected cells were treated with or without 100 μM diazoxide (DZX). FP oxidation (%) was calculated as a percentage of the 100 μM DNP-induced fluorescence. Data shown are representative of four separate experiments. (**b**) Effect of transfection of PKC-ε on diazoxide-induced maximum flavoprotein (FP) oxidation. The PKC-ε transfected cells were treated with or without 100 μM diazoxide. FP oxidation (%) was calculated as a percentage of the 100 μM DNP-induced fluorescence. The data are mean±s.d. (*n*=4). *$P<0.05$ vs pcDNA alone, #$P<0.05$ vs diazoxide-treated pcDNA. (**c**) Effect of PKC-ε inhibitor (εV1–2) and mitoK$_{ATP}$ channel inhibitor (5-HD) on PKC-ε overexpression-induced maximum flavoprotein (FP) oxidation. The PKC-ε transfected cells were treated with 100 μM diazoxide in the absence or presence of 10 μM εV1–2 or 100 μM 5-HD. The data are mean±s.d. (*n*=4). *$P<0.05$ vs vehicle-treated PKC-ε WT, #$P<0.05$ vs PKC-ε WT.

opening (Figure 7a and b), it is suggested that hypoxia-induced disruption of Δψ$_m$ may not be caused by PTP in H9c2 cells. As demonstrated in our previous results, hypoxia-induced disruption of Δψ$_m$ reaches a peak at 4 h of hypoxia (Kim *et al.*, 2005) and the cytochrome *c* release into cytosol reaches a peak at 6 h of hypoxia (Figure 8c). From these results, it is suggested that the disruption of Δψ$_m$ by hypoxia-
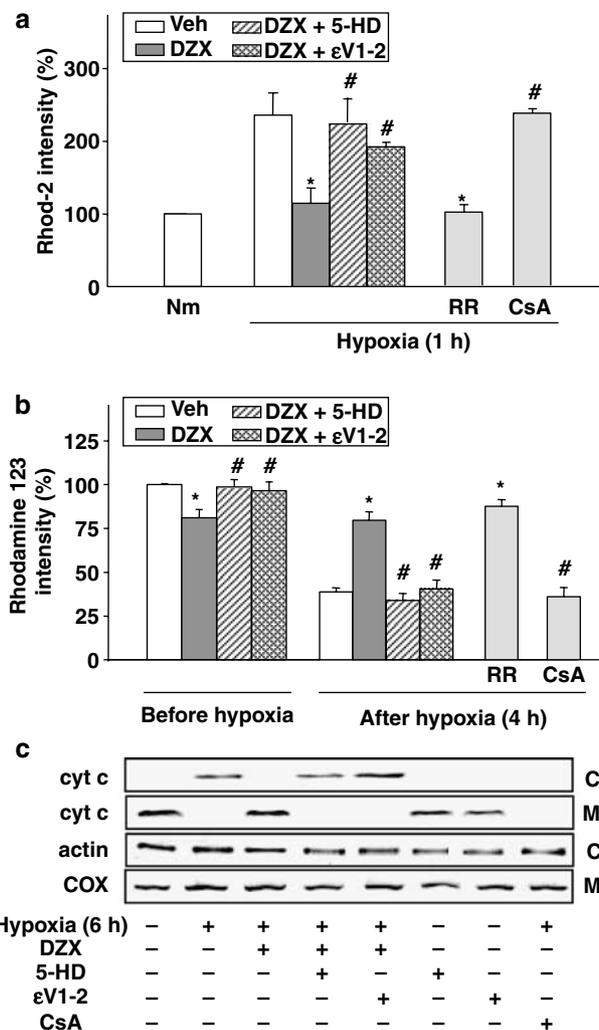
Figure 8 The role of PKC-ε in diazoxide-induced inhibitory effect on mitochondrial death pathway. The cells were treated with 100 μM diazoxide (DZX) for 1 h before and during hypoxia in the absence or presence of PKC-ε inhibitor (εV1–2) or K$_{ATP}$ channel inhibitor (5-HD). (**a**) Effect of 10 μM εV1–2 and 100 μM 5-HD on diazoxide-induced attenuation of mitochondrial Ca^{2+} ([Ca^{2+}]$_{mito}$) overload during hypoxia. Quantitative analysis of rhod-2 intensity after 1 h of hypoxia. Data shown as means±s.d. (*n*=5) represent the percentage of the vehicle-treated normoxic control (Nm). *$P<0.05$ vs vehicle-treated hypoxic control (Veh). #$P<0.05$ vs diazoxide alone (DZX). RR, Ruthenium Red; CsA, cyclosporin A. (**b**) Effect of 10 μM εV1–2 and 100 μM 5-HD on reduction of mitochondrial membrane potential (Δψ$_m$). Δψ$_m$ was determined by FACScan analysis of rhodamine 123 intensity after 4 h of hypoxia. Data shown as means±s.d. (*n*=4) represent the percentage of the vehicle-treated normoxic control. #$P<0.05$ vs vehicle-treated control (Veh). *$P<0.05$ vs DZX alone. RR, Ruthenium Red; CsA, cyclosporin A. (**c**) Effect of 10 μM εV1–2 and 100 μM 5-HD on diazoxide-induced cytochrome *c* release during hypoxia. Western blots for cytochrome *c* detected in the cytosolic (C) and the mitochondrial (Mt) fractions after 6 h of hypoxia. Blots shown are representative of four separate experiments. CsA, cyclosporin A; COX, cytochrome *c* oxidase subunit IV.

induced [Ca^{2+}]$_{mito}$ overload may cause PTP opening and subsequently cytochrome *c* release in cardiomyocytes. Mitochondrial Ca^{2+} overload and the large reduction in Δψ$_m$ during hypoxia were markedly attenuated by diazoxide in the 'pre/during' treatment group (Figure 8a and b). Taking

into consideration that the driving force responsible for the mitochondrial Ca^{2+} uptake through the Ca^{2+} uniporter is the difference in $\Delta\psi_m$ across the inner mitochondrial membrane (Smaili *et al.*, 2003), the present results strongly support the previous notion that mitoK$_{ATP}$ channel opening by diazoxide partially depolarizes $\Delta\psi_m$ before hypoxia and thus might attenuate the massive overload of mitochondrial Ca^{2+} during hypoxia by decreasing the driving force for mitochondrial Ca^{2+} uptake (Holmuhamedov *et al.*, 1998). Our results further demonstrated that inhibitory effects of diazoxide on hypoxia-induced increase in $[Ca^{2+}]_{mito}$ and reduction in $\Delta\psi_m$, as well as hypoxia-induced cytochrome *c* release and cell death, were almost completely abolished by εV1–2 as well as 5-HD. These results indicate that diazoxide-induced cardioprotection involving modulation of the mitochondrial death pathway is mediated through activation of PKC-ε as well as the mitoK$_{ATP}$ channel opening, although further studies on the mitochondrial death pathway need to be performed with neonatal rat cardiomyocytes because these results were obtained from H9c2 cells (Figure 8).

Taken together, the present results suggest a signaling pathway by which diazoxide induces mitoK$_{ATP}$ channel opening mediated through PKC-ε activation, leading to cardioprotection. There have been several reports suggesting that PKC is an upstream signaling molecule of mitoK$_{ATP}$ channel (Ohnuma *et al.*, 2002; Hassouna *et al.*, 2004), which appears to be similar to our results, at a first glance. These studies, however, were quite different from ours because they were carried out on the assumption that diazoxide is a direct activator of the mitoK$_{ATP}$ channel, and suggested a signal transduction sequence of PKC→diazoxide-induced direct activation of the mitoK$_{ATP}$ channel. On the other hand, our study suggests an indirect signaling pathway for the action of diazoxide on the mitoK$_{ATP}$ channel opening, that is, diazoxide→PKC-ε→mitoK$_{ATP}$ channel→$\Delta\psi_m$ reduction. Although it is not clear how PKC-ε translocation induces opening of the mitoK$_{ATP}$ channel, it is possible that PKC-ε translocated to the mitochondria by diazoxide regulates activity of the mitoK$_{ATP}$ channel, possibly by phosphorylation of a relevant protein (Light *et al.*, 2000).

In summary, the results from this study suggest that diazoxide may be acting more as a PKC-ε activator than a direct mitoK$_{ATP}$ channel opener in H9c2 cells lines and neonatal rat cardiomyocytes. Further studies should be investigated whether diazoxide can directly modulate the recombinant PKC-ε *in vitro*, which would add evidence for the potential use of diazoxide as a specific PKC-ε activator.

Acknowledgements

Conflicts of interest

The authors state no conflict of interest.

References

Akao M, O'rourke , Kusuoka H, Teshima Y, Jones SP, Marban E (2003). Differential actions of cardioprotective agents on the mitochondrial death pathway. *Circ Res* **92**: 195–202.

Anderson CD, Pierce J, Nicoud I, Belous A, Knox CD, Chari RS (2005). Modulation of mitochondrial calcium management attenuates hepatic warm ischemia-reperfusion injury. *Liver Transpl* **11**: 663–668.

Baines CP, Zhang J, Wang GW, Zheng YT, Xiu JX, Cardwell EM *et al.* (2002). Mitochondrial PKCε and MAPK from signaling modules in the murine heart. *Circ Res* **90**: 390–397.

Costa AD, Garlid KD, West IC, Lincoln TM, Downey JM, Cohen MV *et al.* (2005). Protein kinase G transmits the cardioprotective signal from cytosol to mitochondria. *Circ Res* **97**: 329–336.

Disatnik MH, Isatnik MH, Buraggi G, Mochly-Rosen D (1994). Localization of protein kinase C isozymes in cardiac myocytes. *Exp Cell Res* **210**: 287–297.

Emaus RK, Grunwald R, Lemasters JJ (1986). Rhodamine 123 as a probe of transmembrane potential in isolated rat-liver mitochondria: spectral and metabolic properties. *Biochim Biophys Acta* **850**: 436–448.

Grimmsmann T, Rustenbeck I (1998). Direct effects of diazoxide on mitochondria in pancreatic B-cells and on isolated liver mitochondria. *Br J Pharmacol* **123**: 781–788.

Gunter TE, Gunter KK, Sheu SS, Gavin CE (1994). Mitochondrial calcium transport: physiological and pathological relevance. *Am J Physiol* **267**: C313–C339.

Hassouna A, Matata BM, Galinanes M (2004). PKC-ε is upstream and PKC-á is downstream of mitoK$_{ATP}$ channels in the signal transduction pathway of ischemic preconditioning of human myocardium. *Am J Physiol Cell Physiol* **287**: C1418–C1425.

Hausenloy D, Wynne A, Duchen M, Yellon D (2004). Transient mitochondrial permeability transition pore opening mediates preconditioning-induced protection. *Circulation* **109**: 1714–1717.

Hescheler J, Meyer R, Plant S, Krautwurst D, Rosenthal W, Schultz G (1991). Morphological, biochemical, and electrophysiological characterization of a clonal cell (H9c2) line from rat heart. *Circ Res* **69**: 1476–1486.

Holmuhamedov EL, Jovanovic S, Dzeja PP, Jovanovic A, Terzic A (1998). Mitochondrial ATP-sensitive K^+ channels modulate cardiac mitochondrial function. *Am J Physiol* **275**: H1567–H1576.

Jung YS, Jung YS, Kim MY, Kim MH, Lee S, Yi KY *et al.* (2003). KR-31466, a benzopyranylindol analog, attenuates hypoxic injury through mitochondrial K$_{ATP}$ channel and protein kinase C activation in heart-derived H9c2 cells. *J Pharmacol Sci* **92**: 13–18.

Kim MH, Jung YS, Moon CH, Jeong EM, Lee SH, Baik EJ *et al.* (2003). Isoform-specific induction of PKC-ε by high glucose protects heart-derived H9c2 cells against hypoxic injury. *Biochem Biophys Res Commun* **309**: 1–6.

Kim MJ, Moon CH, Kim MY, Lee S, Yi KY, Yoo SE *et al.* (2005). KR-32570, a novel Na^+/H^+ exchanger-1 inhibitor, attenuates hypoxia-induced cell death through inhibition of intracellular Ca^{2+} overload and mitochondrial death pathway in H9c2 cells. *Eur J Pharmacol* **525**: 1–7.

Lee YJ, Soh JW, Jeoung DI, Cho CK. Jhon GJ, Lee SJ, Lee YS (2003). PKC-ε-mediated ERK1/2 activation involved in radiation-induced cell death in NIH3T3 cells. *Biochim Biophys Acta* **1593** (2–3): 219–229.

Light PE, Bladen C, Winkfein RJ, Walsh MP, French RJ (2000). Molecular basis of protein kinase C-induced activation of ATP-sensitive potassium channels. *Proc Natl Acad Sci USA* **97** (16): 9058–9063.

Liu Y, Sato T, O'rourke B, Marban E (1998). Mitochondrial ATP-dependent potassium channels: novel effectors of cardioprotection? *Circulation* **97**: 2463–2469.

Liu H, Zhang HY, Zhu X, Shao Z, Yao Z (2002). Preconditioning blocks cardiocyte apoptosis: role of K$_{ATP}$ channels and PKC-ε. *Am J Physiol Heart Circ Physiol* **282**: H1380–H1386.

Moon CH, Kim MY, Kim MJ, Kim MH, Lee S, Yi KY *et al.* (2004). KR-31378, a novel benzopyran analog, attenuates hypoxia-induced cell death via mitochondrial K_{ATP} channel and protein kinase C-ε in heart-derived H9c2 cells. *Eur J Pharmacol* **506**: 27–35.

Murata M, Akao M, O'rourke B, Marban E (2001). Mitochondrial ATP-sensitive potassium channels attenuate matrix Ca^{2+} overload during simulated ischemia and reperfusion: possible mechanism of cardioprotection. *Circ Res* **89**: 891–898.

Ohnuma Y, Miura T, Miki T, Tanno M, Kuno A, Tsuchida A *et al.* (2002). Opening of mitochondrial K_{ATP} channel occurs downstream of PKC-ε activation in the mechanism of preconditioning. *Am J Physiol Heart Circ Physiol* **283**: H440–H447.

Sato T, O'rourke B, Marban E (1998). Modulation of mitochondrial ATP-dependent K^+ channels by protein kinase C. *Circ Res* **83**: 110–114.

Schafer G, Wegener C, Portenhauser R, Bojanovski D (1969). Diazoxide, an inhibitor of succinate oxidation. *Biochem Pharmacol* **18**: 2678–2681.

Simkhovich BZ, Przyklenk k, Kloner RA (1998). Role of protein kinase C as a cellular mediator of ischemic preconditioning: a critical review. *Cardiovasc Res* **40**: 9–22.

Smaili SS, Hsu YT, Carvalho AC, Rosenstock TR, Sharpe JC, Youle RJ (2003). Mitochondria, calcium and pro-apoptotic proteins as mediators in cell death signaling. *Braz J Med Biol Res* **36**: 183–190.

Trollinger DR, Cascio WE, Lemasters JJ (1997). Selective loading of Rhod 2 into mitochondria shows mitochondrial Ca^{2+} transients during the contractile cycle in adult rabbit cardiac myocytes. *Biochem Biophys Res Commun* **236**: 738–742.

Wang S, Cone J, Liu Y (2001a). Dual roles of mitochondrial K_{ATP} channels in diazoxide-mediated protection in isolated rabbit hearts. *Am J Physiol Heart Circ Physiol* **280**: H246–H256.

Wang Y, Ashraf M (1999). Role of protein kinase C in mitochondrial K_{ATP} channel-mediated protection against Ca^{2+} overload injury in rat myocardium. *Circ Res* **84**: 1156–1165.

Wang Y, Hirai K, Ashraf M (1999). Activation of mitochondrial ATP-sensitive K^+ channel for cardiac protection against ischemic injury is dependent on protein kinase C activity. *Circ Res* **85**: 731–741.

Wang Y, Takashi E, Xu M, Ayub A, Ashraf M (2001b). Downregulation of protein kinase C inhibits activation of mitochondrial K_{ATP} channels by diazoxide. *Circulation* **104**: 85–90.

Zaugg M, Lucchinetti E, Spahn DR, Pasch T, Garcia C, Schaub MC (2002). Differential effects of anesthetics on mitochondrial K_{ATP} channel activity and cardiomyocyte protection. *Anesthesiology* **97**: 15–23.

*BJP***Open**   This article is available free of charge on the BJP website (http://www.brjpharmacol.org).